Numerical Modeling of Explosively Loaded Concrete Structure Using a Coupled CFD-CSD Methodology

Michael E. Giltrud[1], Joseph D. Baum[2], Orlando A. Soto[3], Fumiya Togashi[4] and Rainald Löhner[5]

[1] *Applied Simulations Inc., 10001 Chartwell Manor Ct., Potomac, MD 20854, USA*
(mike.giltrud@appliedsimulations.com)
[2] *Applied Simulations Inc., 10001 Chartwell Manor Ct., Potomac, MD 20854, USA*
(joseph.d.baum@appliedsimulations.com)
[3] *Applied Simulations Inc., 10001 Chartwell Manor Ct., Potomac, MD 20854, USA*
(orlando.a.soto@appliedsimulations.com)
[4] *Applied Simulations Inc., 10001 Chartwell Manor Ct., Potomac, MD 20854, USA*
(fumiya.togashi@appliedsimulations.com)
[5] *George Mason University, Fairfax, VA 22030, USA*
(rlohner@gmu.edu)

This paper describes the application of a state-of-the-art coupled computational fluid dynamics (CFD) and computational structural dynamics (CSD) methodology to the simulation of an explosively loaded reinforced concrete structure that was loaded to destruction. The objective of the study was to predict the response of the structure, initial debris launch and pressure response within and external to the structure for four differing load cases.

The subject of this study was a joint Norwegian and Swedish experimental program, completed in 2008, that examined the detonation of explosives within concrete structures and the lethal debris thrown out to large distances. This debris can often be the most important hazard parameter following an accidental detonation. This was the third in a series of such tests and is known as The Kasun-III test series. The test structures were small reinforced concrete cubes having internal dimensions of 2.0 by 2.0 by 2.0 meters.

Four different load cases consisting of both cased and bare charges were selected to assess the effectiveness of a coupled CFD-CSD simulation. The simulation must address HE initiation, detonation wave propagation through the HE, air blast impact on the concrete structure and initial structural response, subsequent structural failure and debris launch, and propagation of air blast to the far field. Over the last several years we have developed a numerical methodology that couples state-of-the-art CFD and CSD methodologies. The flow code solves the time-dependent, compressible Euler and Reynolds-Averaged Navier-Stokes equations on an unstructured mesh of tetrahedral elements. The CSD code solves explicitly the large deformation, large strain formulation equations on an unstructured grid composed of bricks and hexahedral elements. The codes are coupled via a 'loose coupling' approach which decouples the CFD and CSD sets of equations and uses projection methods to transfer interface information between the CFD and CSD domains.

The results of the simulations generally compare well with the experimental data. The predicted initial structural disassembly agrees well with the initial high speed photography. The predictions exhibit similar failure mechanisms, failure locations and times of failure. The far field pressures exhibit similar decay with range as the experimental data though the pressure is slightly higher. Finally the initial structural debris launch velocity follows that of the experiment.

Keywords: CFD, CSD, Airblast, Wall Breach, Blast Propagation

1.0 Introduction

Munition storage may cause significant damage to the surrounding area if an accident occurs within the storage containers. The damage to the surroundings is usually caused by air blast, debris and fire caused by the accidental explosion. To avoid damage to facilities and injuries to personnel, it is necessary to establish safe stand-off areas around the storage.

In 2008 a joint Norwegian and Swedish experimental program was completed that examined the detonation of explosives within concrete ammunition storage structures. The program focused on pressure occurring from detonation and the debris thrown out to large distances.

This was the third in a series of experiments. Two previous test series, Kasun-I [1] and Kasun-II [2] focused on the breakup, debris formation and debris dispersion from the use of uncased explosives in a small cubical shaped concrete building, now commonly known as a "Kasun".

The Kasun-III test series comprised five tests with 1, 4 and 16 155 mm artillery shells in three separate tests and 6.9 kg and 110 kg bare plastic explosives as two reference tests. All five tests were with charges located inside the Kasun structure. The tests were instrumented with pressure gauges inside and outside the structure. There was an extensive debris recovery effort to understand the debris caused by the detonations.

To aid in the analysis and understanding of the tests computational tools will be applied to analyze the tests. Computational tools have evolved significantly over the last decade. Today, coupled computational structural dynamics (CSD) and computational fluid dynamics (CFD) codes are available and are suitable for this problem set. The objective of this paper is to assess the suitability of a coupled CSD/CFD code to predict the air blast, structural response and damage and debris throw from a detonation of a munition storage container. Four tests consisting of 1 and 16, 155 mm artillery shells in two separate tests and 6.9 kg and 110 kg bare plastic explosives as two reference tests from the 2008 joint Norwegian and Swedish test series were selected for the evaluation exercise.

2.0   Experimental Configuration

The test structure has a door with a 0.5 cm steel outer plate and a 0.2 cm steel plate as inner plate having a total thickness of 21 cm. The door has a total weight of approximately 350 kg/m^2. The door opening is 170 cm high and 90 cm wide. The door was closed in all the tests by 3, 2.5 cm steel lock cylinders and 2, 2.5 cm hinge bolts. Figure 1 from [3] gives the configuration of the test articles.

The experimental program involved both cased (155 mm artillery shells) and uncased charges. The 155mm shells contains 6.7 kg of TNT and a 42 kg steel case. The uncased charge were made of a PETN based plastic bonded high explosive consisting of 85 % PETN and 15 % mineral oil. The charge was cylindrical with a length to diameter ratio of 6. The charge had a diameter of 10 cm and a height of 60 cm. Each cylinder contained 6.9 kg of the PETN based explosive. The charges were elevated off the floor by 15 cm. The loading density of the Kasun III structure for this a single charge was 0.9 kg /m^3. For the multi-charge loading case, consisting of sixteen individual charges, the loading density was 14.4 kg /m^3.

All tests were instrumented with ten external free field pressure gauges. The pressure gauges were located at 20, 30, 40 and 80 m distances along two radials. One radial projected from one side and the other one projected from the back of the Kasun structure. In addition, there were six pressure gauges located inside

the structure on the side wall. The objective of the internal pressure measurements was to determine the internal blast loads on the walls of the concrete structures.

Figure 1 Kasun III Structure

The internal pressure transducers were specially designed and constructed by TNO for the near source explosive environment [4]. The pressure gauges were carbon resistive transducers. For the protection against the fragments and debris, the measuring element of transducers was partially covered with a 1.0 cm thick arch shaped piece of steel.

2.0 Computational Strategy

Any blast-structure simulation proceeds through the following stages: 1. Pre-Processing; 2. Grid Generation; 3. Coupled Fluid/Structure Solver; and 4. Post-Processing

Automatic unstructured mesh surface and volume generation has reached a high level of maturity over the past several years. The graphic pre-processor FECAD [5] enables the preparation of the data sets for the solver and the mesh generator FRGEN3D. It also quickly generates CSM meshes from existing CFD domains, thereby easing the process of setting up a complex-geometry coupled problem [6,7].

Mesh generation for both the CSM and CFD is performed using FRGEN3D [8,9]. This unstructured grid generator is based on the advancing front method. The CFD mesh is composed of triangular (surface) and tetrahedral (volume) elements. The CSM mesh includes beams, triangular or quad shells and bricks or hexahedra (solids). Although the angles of a typical hex are less than perfect, extensive testing against perfect-angle bricks for both linear and nonlinear cases produced almost identical results. This, nevertheless, necessitated the replacement of the Belytschko-Tsay hourglass control model (default model in DYNA3D [10], with the Flanagan-Belytschko hourglass control model (model no. 3 in DYNA3D), incurring a 30% performance penalty.

The flow solver employed is FEFLO, a 3-D adaptive, unstructured, edge-based hydro-solver based on the Finite-Element Method Flux-Corrected Transport (FEM-FCT) [11]. It solves the Arbitrary Lagrangean-Eulerian (ALE) formulation of the Euler and Reynolds-averaged turbulent, Navier-Stokes equations. In addition to the more mature, FEM-FCT, several shock capturing features have been added over the years: Rieman solvers with a choice of limiters, Roe solvers [12], high-order (to eight) ENO schemes [13], and the latest Discontinuous Galerkin solvers [14].

The spatial mesh adaptation is based on local H-refinement, where the refinement/deletion criterion is a modified H2-seminorm [15] based on user-specified unknowns. Equations of state (EOS) supported by FEFLO include ideal polytropic gas, real air EOS table look-up, water EOS table look-up, a link to the SESAME library of EOS, and the JWL EOS and several afterburning and combustion models [16,17]. Flows with particles are treated via a second solid phase. The particles interact with the fluid, exchanging mass, momentum and energy, and are integrated in a time-consistent manner with the fluid. Flows with multiple moving bodies are handled using an embedded approach [18].

The CSD code is ASICSD, a new CSD code intended to model large structural deformations [19,20]. This is an unstructured, explicit finite element code, well suited for modeling large deformations. It provides a good base for non-linear materials with elasto-plastic compartmental laws with rupture. The code incorporates a large library of materials and various equations-of-state, as well as many kinematic options, such as slide-lines and contacts. ASICSD models the weapon detonation/fragmentation, as it can model case cracking (thermal softening was defined by the Johnson and Cook model). ASICSD solves the continuous mechanics equilibrium equation. The weak formulation (virtual work principle) is written in the spatial configuration (actual configuration) and it is discretized in time using an explicit second-order central difference scheme.

In space, the virtual work equation is solved by using stable finite element types. The most commonly used elements are: a fully integrated large-deformation Q1/P0 solid element (hexahedra with an 8 nodes interpolation scheme for the kinematic variables and constant pressure) which does not present hourglass modes and does not lock for incompressible cases. Several 3-node and 4-node large-deformation shell elements (Hughes-Liu shell, Belytschko shells, MITC shells, ASGS stabilized shells) which are formulated using standard objective stress update schemes (Jaumann-Zaremba, co-rotational embedded axis, etc,), are fully integrated to avoid hourglass spurious modes. Finally, some objective truss and beam elements (i.e. Belytschko and Hughes-Liu beams) have also been implemented.

Many different material models have been included into the code. The most commonly used are: a plasticity model which relies on a hyper-elastic characterization of the elastic material response for the solid elements, and a standard hypo-elastic plasticity model for the shell, beam and truss elements. The most often used failure criterion is based on the maximum effective plastic strain and the stress tensor inside the element. The fracture may be simulated by element erosion and/or node disconnection. The code is fully parallelized using both OpenMP and MPI directives. The code has been extensively validated [21].

Coupling between all modules is provided by FEMAP, via a loose-coupling approach. The embedded approach is used to couple the CFD and CSM module.
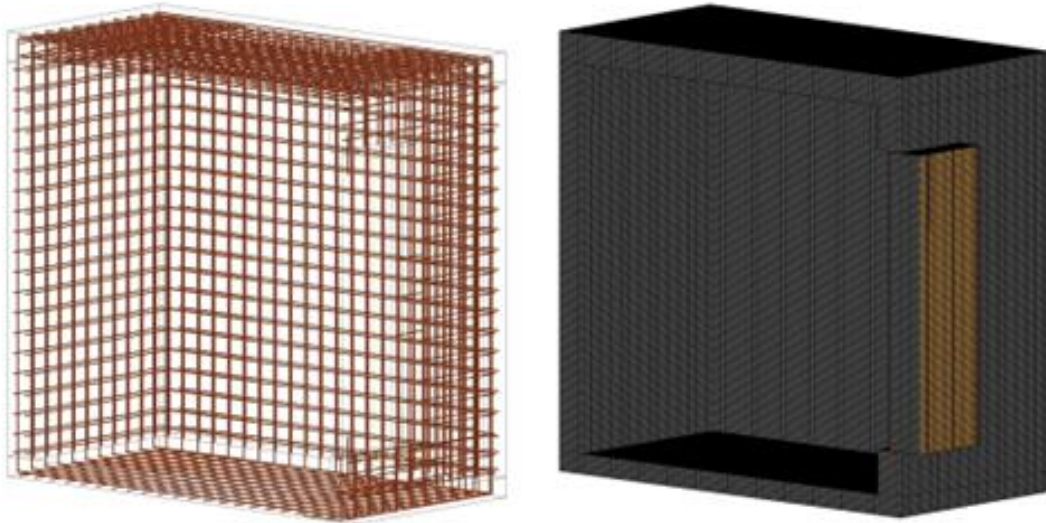
3.0 Computational Model

For all four loading cases, the simulation must address the explosive initiation and detonation, detonation wave propagation through the HE. The simulation must also calculate the air blast propagation and impact on the concrete structure, initial structural response, subsequent structural failure and debris launch, and propagation of air blast to the far field.

To accomplish this, first a finite element model of the charge is constructed. The four cases under consideration are a single bare charge a single 155mm cased charge, 16, bare charges and 16, 155 mm cased charges. Owing to symmetric considerations, half symmetry was applied to the problem. A vertical plane passing thru the charge defined the plane of symmetry for the single charge case. For the cases of

4

sixteen charges a vertical plane of symmetry passing between the two groups of eight charges defined the plane of symmetry. Half symmetry reduced the problem size while retaining any three dimensional effects that might occur during the initial detonation and blast propagation.

A finite element model of the Kasun structure was constructed. The reinforcing was modeled explicitly and is shown in Figure 2(a). Each reinforcing bar is modeled as beam element. The finite element model of the Kasun structure is shown in Figure 2(b) without the door attached. The mesh was essentially uniform with an average element size of 1.25 cm, allowing 12 elements thru the thickness of the wall. This level of refinement provided adequate detail to model the response of the walls and roof of the structure. The concrete has a compressive strength of 48 MPa. The K&C concrete model was used to model the concrete non-linear response [22,23].

(a)   (b)

Figure 2 Kasun Finite Element Model

The door was modeled as two plates sandwiching the concrete in-fill. The outer plate was 0.5 cm thick and the inner plate was 0.2 cm thick total thickness of the door was 21 cm. The weight of the door was 350 kg/m². The door's 3 lock cylinders were modeled as beams and the 2 hinge bolts were modeled as beams. The initial early time computational grid consisted of 220 million fluid/explosive elements and 820,000 structural elements in a 6 m x 3.5 m x 6.25 m (l x w x h) computational volume. The charge was initiated.

4.0 Computational Results

4.1 Single Bare Charge

The detonation ran through the explosive, the shock wave formed and ran through the air inside the structure, hit the interior walls of the structure and reflected loading the interior of the walls. The waves reflected numerous times insides the structure causing the structure to respond and begin to sustain damage in the form of high stress and cracking at the wall-floor interfaces and lower part of the vertical corners, all within the first few milliseconds.

As was mentioned previously, six pressure gauges were mounted on the interior wall of the structure. The goal of the gauges was to measure the loads on the structure. We calculated the pressures at each of the pressure gauges. The comparisons of two representative pressure gauges are shown below in Figure 3.

For pressure gauge P3, the lower left gauge, the calculated peak pressure is less than that measured. The second peak is quite well represented and the rest of the record follows reasonable well. The impulse is also within about 15% of the experimental value. For pressure gauge P4, the upper right gauge, the calculated peak pressure is very accurate to that measured. The first half of the record represents the experiment quite well, however, after that the calculated record is out of phase with the experimental record. The peak impulse predicted very well.

P3 Lower Left   P4 Upper Right

——— Experimental Pressure
——— Experimental Impulse
——— Calculated Pressure
——— Calculated Impulse

Figure 3 Single Bare Charge – Internal Pressure Comparison

The structure has undergone significant loading and damage by 10 msec. Figure 4 shows the deformed state comparing it to a frame from the high speed video. The high speed video shows the structure venting detonation products from the connection between the wall and the floor, the vertical connection between the walls and the connection between the roof and the walls. This suggests that the wall has cracked all the way through allowing the gasses to escape.

The finite element model has similar results. The model has separated at the wall-floor and the wall-roof interfaces. The wall extends beyond the floor and roof perimeter. Also the reinforcing has begun to pull out of the roof and the floor. In fact, examining the reinforcing shows that the reinforcing has broken at the floor wall interface. The model has a very distinct separation between the vertical walls extending nearly the entire length of the wall. Examining the reinforcing shows that the horizontal reinforcing has broken about half way up the structure.
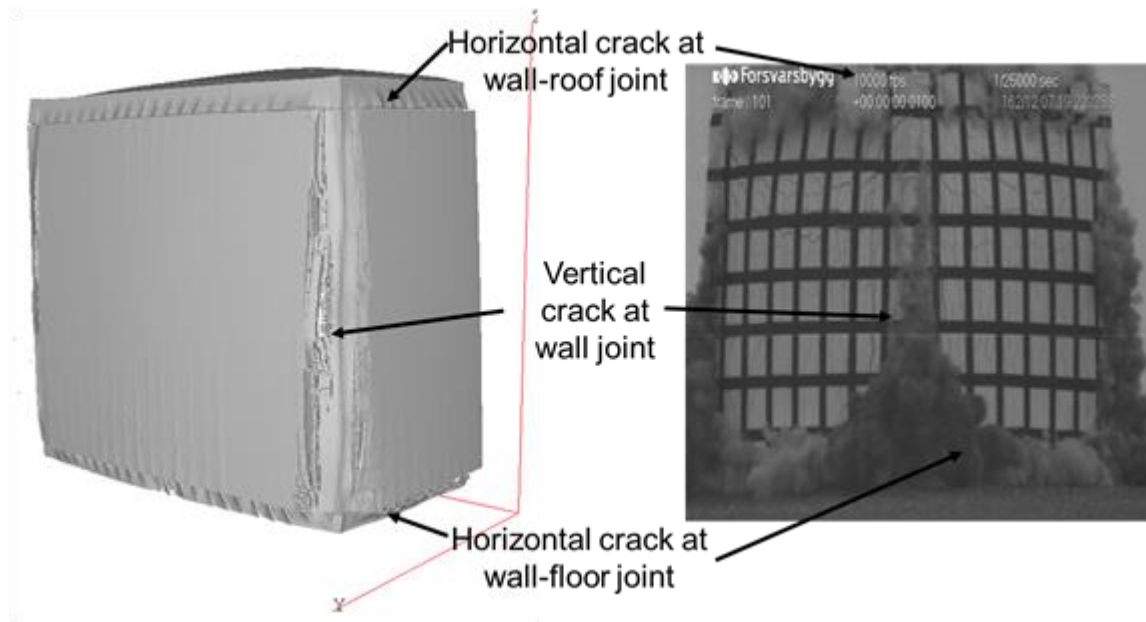
6

Figure 4 Single Bare Charge – *Damage of the Kasun Structure at 10 msec.*

The pressure waves propagated from the Kasun into the far field. To measure the pressure in the far field, there were pressure gauges fielded along two radials, the side and the back of the Kasun at 20m, 30m, 40m, and 80m range. We calculated the pressure into the far field to nearly 30 m range. The peak pressure vs range is shown in Figure 5 for pressure along the side radial and the back radial.

The peak pressure along both the side and back radials appears to have the correct attenuation however the prediction are about 2 kPa higher than the measured data. There are a couple of reasons to explain this phenomena. First the finite element model might disassemble more quickly than the experimental one causing the blast wave to escape at a higher initial value. Another possibility is that the experimental structure might have broken into more and finer pieces thereby causing the blast wave to propagate through a dustier and debris filled region. Unfortunately the numerical data doesn't provide us enough information to allow us to define the actual cause.
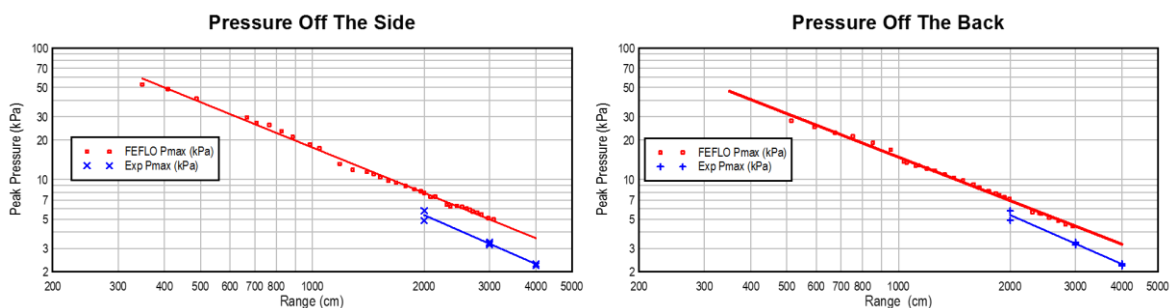

Figure 5 Single Bare Charge – *Pressure versus Range for Two Radials.*

4.2

4.2 Sixteen Bare Charges

The second under consideration consists of 16 bare charges where each charge is a 6.9 kg bare PETN charge as in the first case for a total of 110kg. As with case 1 above the early time internal pressure was compared to the measured pressure. Illustrative examples of the comparison between the prediction and the experiment is shown in Figure 6 below.
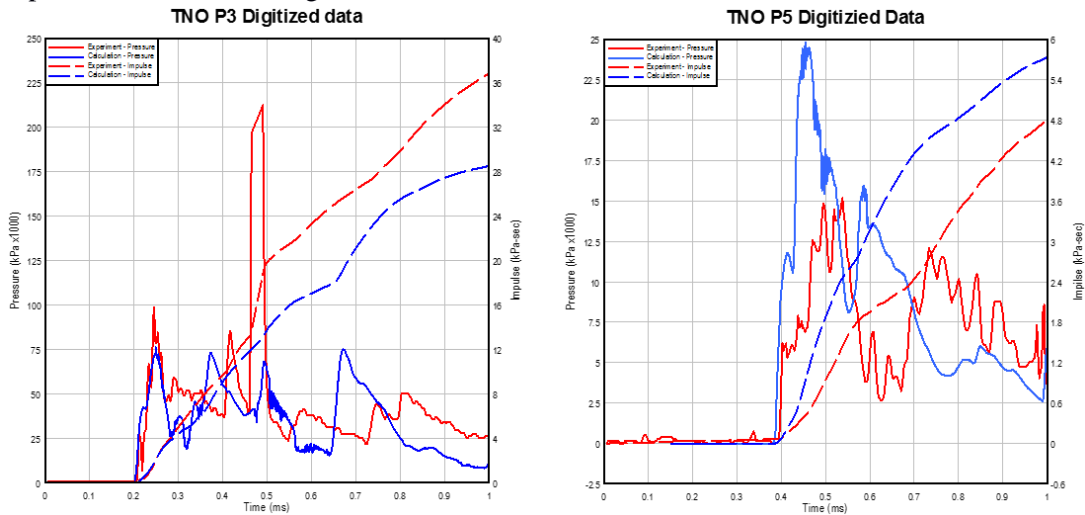

Figure 6 Sixteen Bare Charges – Internal Pressure Examples.

For P3, the initial pressure comparison is generally quite good, matching bothe time of arrival and initial peak amplitude. Unfortunately at 0.5 ms there is a large spike in the experiment the predictions does not exhibit. The impulse tracks well with the experimental impulse except for the large spike. For the other record, the calculated peak is higher than the measured peak and the duration is somewhat longer. The impulses for the two records are within 15%.

Owing to the significantly higher net explosive loading 110kg for this case vice 6.9 kg for the previous case, the structure undergoes damage more rapidly. In fact, by only 2.8 ms the structure is significantly damaged. Figure 7 below compares the calculated deformed structure at 2.8 ms to a frame extracted from the high speed video of the event.
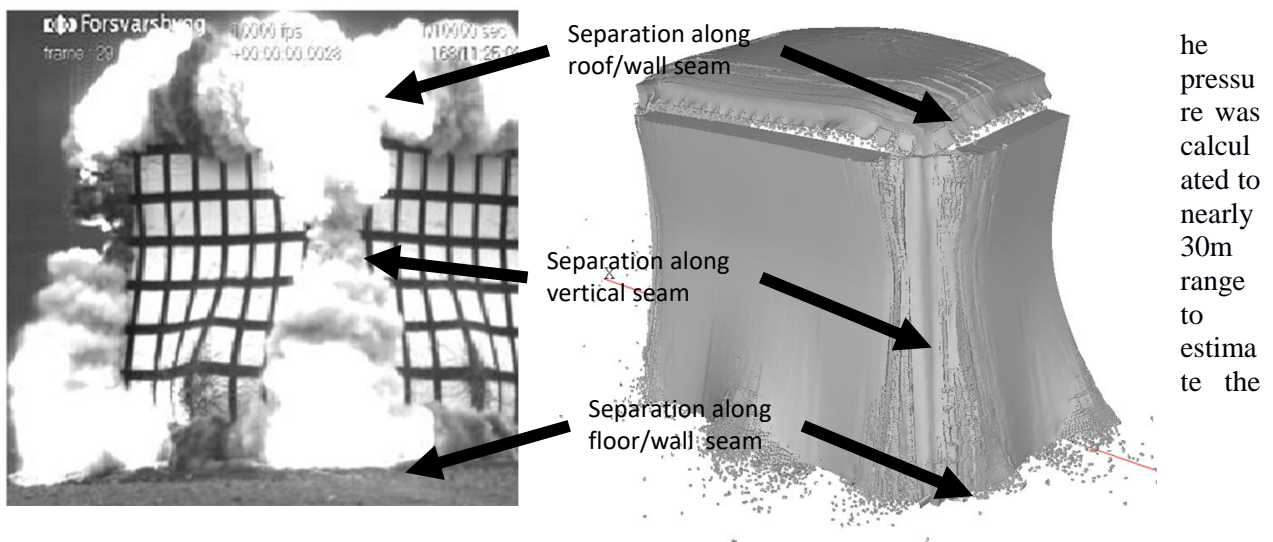

The pressure was calculated to nearly 30m range to estimate the

Figure 7 Sixteen Bare Charges – Damage of the Kasun Structure at 2.8 msec.

far field attenuation. Figure 8 shows the pressure and impulse attenuation for the sixteen bare charge case. The pressure attenuation tracks well with the experimental data. The impulse attenuation will not as far in range is also quite good.
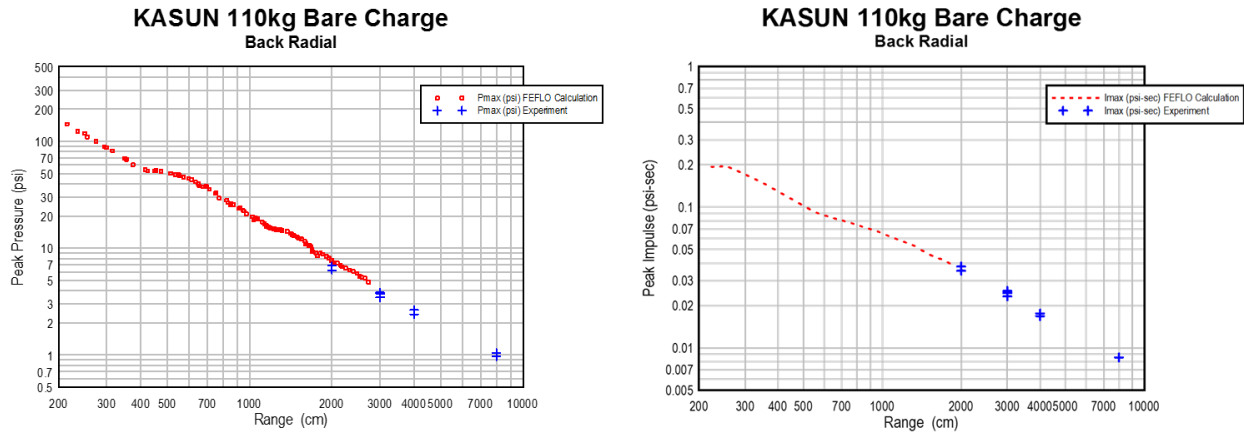

Figure 8 Sixteen Bare Charges – Pressure and Impulse Attenuation.

4.3 One 155mm Cased Charges

To assess the effects of fragments on the structural loading, a single 155mm cased charge was used for the comparison to the experiment. The particular 155mm warhead was the M107 warhead which consists of a 42 kg steel case and a 6.7 kg of TNT charge. The finite element model is shown in Figure 9. The model consists of about 100,000 steel elements. The case was allowed to naturally fragment using a Mott model based on maximum plastic strain.
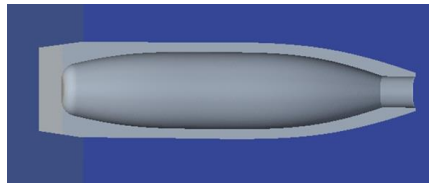

Figure 9 Single Cased Charge – Finite Element Model of 155mm Warhead.

As with the previous two cases, the early time internal pressure was compared to the measured pressure. Illustrative examples of the comparison between the prediction and the experiment is shown in Figure 10 below.
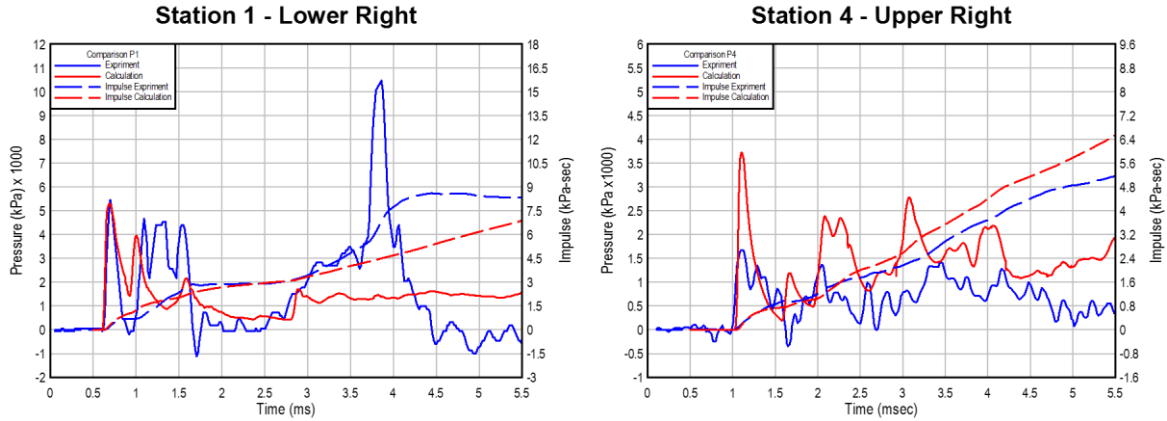
9

Station 1 - Lower Right   **Station 4 - Upper Right**

Figure 10 Single Cased Charge – Internal Pressure Comparisons.

For Station 1, the calculated first peak agrees very well with the experimental value. The second calculated peak is a little early and a little less in magnitude. The calculation misses completely the next two experimental peaks and the large peak at about 4.0 ms. Nevertheless the calculated impulse is within about 15% of the experiment.   For station 4, the calculated first peak is significantly higher than the experimental value. The calculation has that are higher than the experimental peaks and out of phase with the experiment. The impulse is less than 20 higher than the experimental impulse.
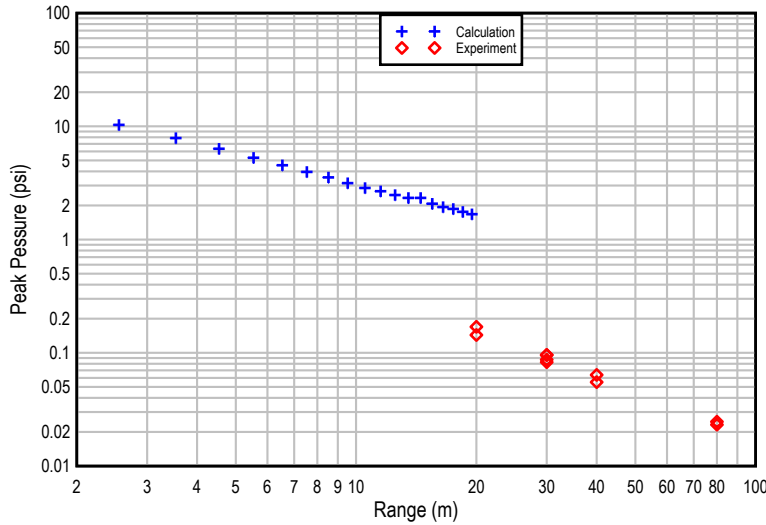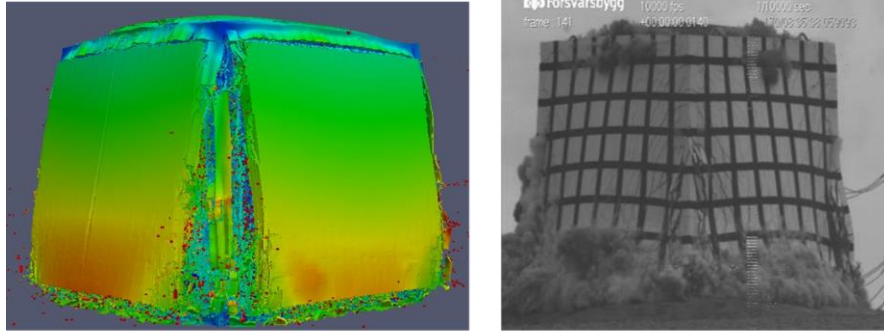
Kasun 1 - 155mm Charge

Figure 11 Single Cased Charge – Pressure Attenuation.

Figure 11 above, provides the pressure attenuation for the case of a single 155mm case charge. While the attenuation generally has the correct trend, it is higher than the experimental attenuation. This is accentuated by the log plot. The actual difference is the attenuation of peak pressures is about 1 psi.

10

Model reproduces:
- Bulging in middle bottom of wall • Crack in corner to roof
- Separation of walls from floor • Initial separation of roof from walls

Figure 12 Single Cased Charge – Structural Deformation at 14.0ms.

Figure 12 shows the comparison of a frame at 14ms from a high speed video compared to the similar calculated result. The model reproduces the bulging in the middle of the bottom wall and the separation of the walls from the floor. The model shows a crack in the vertical seam between the walls running from the floor to the ceiling. The calculation somewhat over accentuates the crack observed in the experimental picture.   Finally, the model shows the initial separation between the roof and the vertical walls.

4.3 One 155mm Cased Charges

The last case that was analyzed consisted of sixteen 155mm warheads detonated inside the Kasun structure.   Each M107 warhead consists of a 42 kg steel case and a 6.7 kg of TNT charge. Therefore the explosive loading was over 107kg of TNT. Figure 13 shows the sixteen M107 155mm warheads inside the Kasun structure. For the calculation, each individual warhead was modeled. Then they were detonated simultaneously.
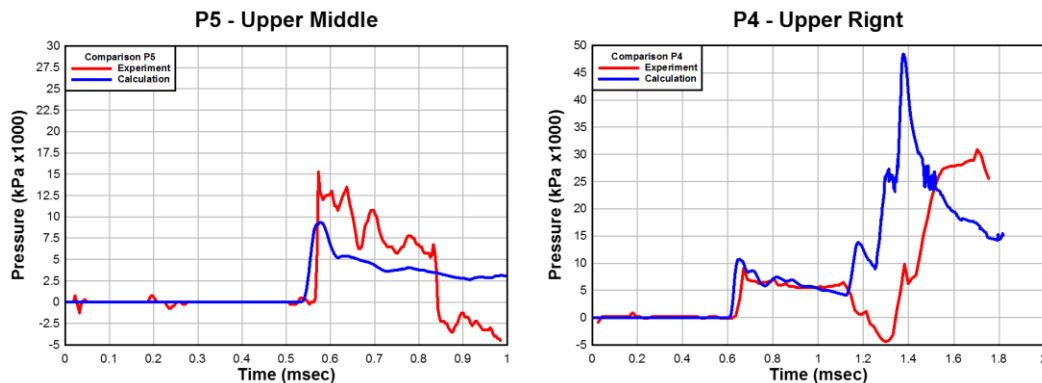

Figure 13 Sixteen Cased Charges.

Figure 14 Sixteen Cased Charge – Internal Pressure.

11

As with the other analyses, the representative results of the early time of the analysis are compared to experimental results. Figure 14 shows illustrative comparison of the calculation to the experiment. The calculation for P5 has about the correct time of arrival but underestimates the peak pressure somewhat. It also fails to reproduce the negative phase occurring at about 8ms. For P4, the early time response is reproduced well. The second peak is early and is higher than the experimental peak.
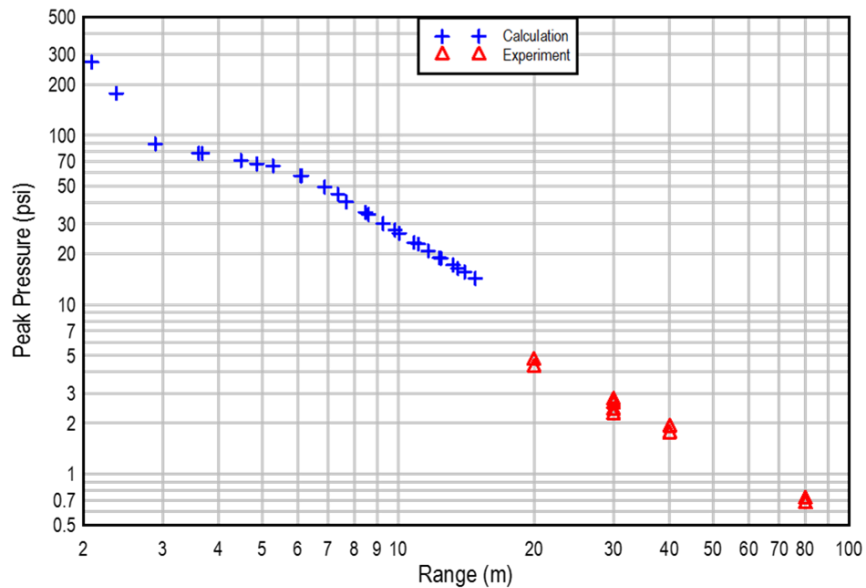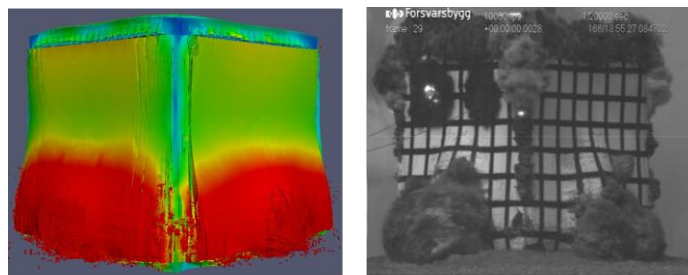

Figure 15 Sixteen Cased Charge – Internal Pressure.

For this case, the pressure was calculated to about 15m in range. The peak pressure attenuation is shown in Figure 15 above. Once again the attenuation represents the experimental attenuation well. It appears that the calculated attenuation will be about 3 psi higher than the measured peak pressure.

Model reproduces:
- Bulging in middle bottom of wall
- Separation of walls from floor
- Crack in corner to mid height
- Initial separation of roof from walls

Figure 16 Sixteen Cased Charge – Damage at 2.8ms.

Figure 16 shows the comparison of a frame at 2.8ms from a high speed video compared to the similar calculated result. The model reproduces the bulging in the middle of the bottom wall and the separation of the walls from the floor. The model shows a crack in the vertical seam between the walls running to the mid height. Finally, the model shows the initial separation between the roof and the vertical walls.

12

5.0 Conclusions

The objective of this paper has been to assess the suitability of a coupled CSD/CFD code applied to the air blast, structural response and damage and debris throw from a detonation of a munition storage container. Tests consisting of 1 and 16, 155 mm artillery shells in two separate tests and 6.9 kg and 110 kg, i.e. sixteen single bare charges, as two reference tests from the 2008 joint Norwegian and Swedish test series were selected for the evaluation exercise. This series spanned a factor of 16 in loading density, i.e. a single charge was 0.9 kg /m^3 and sixteen charges was 14.4 kg /m^3 with and without fragment loading.

There were six pressure gauges were mounted on the interior wall of the structure for each test. The goal of the gauges was to measure the loads on the structure. We calculated the pressures at each of the pressure gauges. Representative pressure comparisons were presented for each case. The pressure and impulse attenuation as a function of range was calculated and compared to the experiment for each case as well. The calculated attenuation generally mirrored the experimental attenuation well though it was somewhat higher than the measured values in some cases.

The deformed state of the finite element model was compared it to a frame from the high speed video. The high speed video shows the structure deforming and in some cases venting detonation products from the connection between the wall and the floor, the vertical connection between the walls and the connection between the roof and the walls. For each case the finite element model showed similar results. While this is not a good quantitative comparison, it does provide qualitative verification that the modeling is reproducing the observed experimental results.

This exercise was begun to build confidence in the use of a coupled CSD/CFD for this application. While the results are not perfect they do begin to demonstrate some confidence that computational tools can generally reproduce experimental results munition storage detonation tests. More comparison to experimental data is still needed to continue to build confidence in this approach.

References

[1]   Langberg, H., Christensen, S. O. & Skudal, S., "Test Program with Small "Kasun" Houses", Forsvarsbygg, FoU Rapport nr. 24/2004.

[2]   Berglund, R., Carlberg, A., Forsén, R., Grönsten, G. A., Langberg, H., "Break up Tests with Small "Ammunition Houses". FOI Report R—2202-SE, Forsvarsbygg Report 51/06, December 2006.

[3]   Grønsten, Geir Arne, Roger Berglund, Anders Carlberg, Rickard Forsén, "Break up Tests with Small "Ammunition Houses" Using Cased Charges - Kasun III". FOI Report R—2749-SE, Forsvarsbygg Report 68/2009, Sept., 2009.

[4]   Van de Kasteele, R.M., "Internal blast pressure measurements during Kasun-3 test series", TNO Defence, Security and Safety, 08 DV03/129, 2008.

[5]   Löhner, R., Yang, C., Cebral, J.R. Soto, O.A., Camelli, F., Baum, J.D., Luo, H., Mestreau, E., and Sharov "Advances in FEFLO"; AIAA-01-0592.

[6]   Baum, J.D., Mestreau, E., Luo, H., Löhner, R., Pelessone, D., Charman, C., "Recent Development of a Coupled CFD/CSD Methodology Using an Embedded Approach."

Proc. 24th Inter. Shock wave Symposium, Beijing, China, July.

[7] Baum, J.D., Soto, O.A., Charman, C., Mestreau, Löhner, R., and Hastie, R., "Coupled CFD/CSD Modelling of Weapon detonation and Fragmentation, and Structural Response to the Resulting Blast and Fragment Loading," NDIA Warhead ballistic conference, Feb 2008, Monterey, CA.

[8] Löhner, R. and P. Parikh, P., "Three-Dimensional Grid Generation by the Advancing Front Method" Int. J. Num. Meth. Fluids 8. 1135-1149.

[9] Löhner, R., "Extensions and Improvements of the Advancing Front Grid Generation Technique," Comm. Num. Meth. Eng. 12, 683-702.

[10] Whirley, R.G. Whirley and Hallquist, J.O., "DYNA3D, A Nonlinear Explicit, Three-Dimensional Finite Element Code for Solid and Structural Mechanics",User Manual; UCRL-MA-107254, also Comp. Meth. Appl. Mech. Eng. 33, 725-757 (1982).

[11] Löhner, R. and Baum, J.D., "Adaptive H-Refinement on 3-D Unstructured Grids for Transient Problems; Int. J. Num. Meth. Fluids 14, 1407-1419.

[12] Löhner, R., Cebral, J.R., Camelli, F.F., Baum, J.D., and Mestreau, E.L, and Soto, O.A., "Adaptive Embedded/Immersed Unstructured Grid Techniques," Arch. Comp. Meth. Eng. 14, 279-301.

[13] Luo, H., Baum, J.D., and Löhner, R., "A Hermite WENO-Based Limiter for DG Methods on Unstructured Grids." AIAA-07-0510.

[14] Luo, H., Baum, J.D. and Löhner, R., "A Discontinuous Galerkin Method Based on a Taylor Basis for the Compressible Flows on Arbitrary Grids." AIAA-07-4080-CP.

[15] Löhner, R. and Baum, J.D., "Adaptive H-Refinement on 3-D Unstructured Grids for Transient Problems; Int. J. Num. Meth. Fluids 14, 1407-1419.

[16] Togashi, F., Löhner, R. and Tsuboi, N., "Numerical Simulation of H2/Air Detonation Using Detailed Reaction Models", AIAA-06-0954.

[17] Togashi, F., Baum, J.D., and Löhner, R., "Numerical Modeling of Aluminum Burning for Heavily Aluminized HE" AIAA-11-3588.

[18] Löhner, R., Baum, J.D., Mestreau, E., Sharov, D., and Charman, C., "Adaptive Embedded Unstructured Grid Methods," Int. J. Num. Meth. Eng., 60, 641-660.

[19] Soto, O.A., Baum, J.D., Löhner, R., Mestreau, E. Luo, H., "A CSD Finite Element Scheme for Coupled Fluid-Solid Problems". Fluid Structure Interaction 2005. September 19-21. La Coruna, Spain.

[20] Soto, O.A., Baum, J.D., Mestreau, E., and Löhner, R., "An Efficient CSD FE Scheme for Coupled Blast Simulations". Ninth US National Congress on Computational Mechanics, San Francisco, CA, July 22-26.

[21] Soto, O.A., Baum, J.D., and Löhner, R.,"An efficient fluid-solid coupled finite element scheme for weapon fragmentation simulations. Eng. Fracture Mech.", Vol 77, 549-564.

[22] Malvar, L.J., Crawford, J.E., Wesevich, J.W., Simons, D.(1997), "A Plasticity Concrete Material Model for DYNA3D," International Journal of Impact Engineering, vol. 19, no. 9/10, Dec. 1997, pp. 847-873.

[23] Malvar, L.J., Crawford, J.E., Wesevich, J.W., Simons, D.(1996), "A New Concrete Material Model for DYNA3D - Release II: Shear Dilation and Directional Rate Enhancements," TM-96-2.1, Report to the Defense Nuclear Agency, Karagozian and Case Structural Engineers, Glendale, CA, January 1996.